Manufacture Porous Materials by Dabco-Based Lonic Liquid

Haleh Sanaeishoar
Azad University: Islamic Azad University
Maryam Sabbaghan (msaba16us@yahoo.com)
Shahid Rajaee Teacher Training University https://orcid.org/0000-0003-4818-8375
Sahar Peimanfar
Azad University: Islamic Azad University

Research Article

Keywords: MCM-41, KIT-1, CTAB, DABCO-based long chain ionic liquid

Posted Date: February 23rd, 2021

DOI: https://doi.org/10.21203/rs.3.rs-227070/v1

Abstract

The long-chain ionic liquid (IL) hexadecyl-4-aza-1-azoniabicyclo[2.2.2]octane bromide was used as a template to prepare the hexagonally ordered siliceous mesoporous molecular sieve MCM-41 as well as the disordered mesoporous molecular sieve designated as KIT-1. The synthesized products were studied via X-ray diffraction (XRD), Fourier transform infrared (FTIR) and N_2 adsorption-desorption analysis. The surface area (BET), pore volume, and pore diameter (BJH) are determined. These kind of ILs that have DABCO (1,4-diazabicyclo[2.2.2]octane) in their structures, were prepared with an easy method. When the two templates, cetyltrimethylammonium bromide (CTAB) and IL, have the similar structures, MCM-41 mesoporous molecular sieve produced with more ordered, uniform mesoporous channel and high surface area in comparison to without IL. When just IL used instead of CTAB, the KIT-1 with non-uniform mesoporous was obtained. Here we prepared the KIT-1 mesoporous molecular sieve with IL without CTAB but it seems, using dual template with changing IL structures in fabricated of molecular sieve provide new opportunity to design targeted adsorbents and catalysis.

1. Introduction

Over the last two decades, the preparation of high surface area mesoporous materials has captured great interest within the scientific community. Much attention has been given lately to various mesoporous silica materials, such as M41S, KIT-1, and SBA-15 [1-3]. These structurally well-defined materials have promising utilizations in catalysis, separation, adsorption, sensing, and delivery of drugs [4-5]. In 1992, mesoporous molecular sieves M41S were discovered by Mobil staff. This outstanding finding has provoked substantial research in this area. One of the most noteworthy mesoporous molecular sieves to mention is MCM-41 which has a hexagonal array of uniform mesoporous[1]. Some innovative templates were used in our former work in pursuance of enhancing the preparatory process [6].

KIT-1 is a noncrystalline molecular sieve that displays short wormlike mesoporous channels. The channels are organized in a disordered three-dimensional system concluded abundant seams. The channel widths, however, are as uniform as the well-ordered mesoporous molecular sieves, MCM-41 [2]. The hydrothermal stability of KIT-I is higher than that of the ordered MCM-41[7]. This kind of molecular sieve reduces probability of channel blockage in their catalytic activity.

There has been much research in recent years into the synthesis methods of MCM-41, [8-11] but only a few studies concerning the synthesis methods of KIT-1. One of these studies was conducted in 1996 by Ryoo et al., and it successfully synthesized KIT-I, for the first time, by an electrostatic templating route by means of ethylenediaminetetraacetic acid tetrasodium salt ($EDTANa_4$), HTAC1, and sodium silicate [2]. Another study was done in 1997 by Ryoo et al. which established another approach to the synthesis of KIT-1 [12]. They synthesis of KIT-1 has been achieved, in the presence of different polyacids, by hydrothermal polymerization of silicate anions surrounding the molecular organization of hexadecyltrimethylammonium chloride [12].

Ionic liquids (ILs), organic salts with low melting points, have been extensively examined and have exceptional characteristics such as extreme stability, high ionic conductivity, non-volatility, adjustable polarity, and recyclability. [13-14] Lately, ILs have been the focus of noticeable consideration not only in chemistry but also in materials science [13]. Specific self-assembled structures can be created with the opportunity of adjustment the amphiphilicity of ILs by modifying the polarizability of the anion and cation or the alkyl chain length. Some researchers in the domain of sustainable green synthesis have paid considerable attention to ILs during the last few decades [15]. ILs were used as template or solvent, in green chemistry, for nanomaterial synthesis [10, 13].

There has been no work in the publications that reports the use of long chain IL based DABCO for mesoporous system synthesis. In the present work, the new IL, hexyldecyl-4-aza-1-azaniabicyclo[2.2.2]octane was synthesized. Structure of used IL is shown in Scheme 1. This structure in compared with CTAB structure is the same long chain and the anion (Scheme 1). The question arises what effect has similarity between CTAB and IL structures used on the mesoporous structure? No work in the literature describes the effect of this IL in mesoporous structure, as far as we know.

In connection with our interest in influence of different ILs as co-template in micro-mesoporous MCM-41 structure and disordered mesoporous material KIT-1, we report here the results of a study on the new IL, hexyldecyl-4-aza-1-azaniabicyclo[2.2.2]octane (**IL-C_{16}**, Scheme 1) with similar structure with CTAB as dual template (**M-1**) and absence of CTAB (**K-1**) [6, 16]. Also, the results were compared with **M-2** as blank sample and **K-2** materials from our previous article [16]. In preparation of **M-2** was used only CTAB as template and **K-2** was used dual template CTAB and dodecyl-4-aza-1-azaniabicyclo[2.2.2]octane (**IL-C_{12}**). The ILs, used in this research, were [C_{16}Dabco]Br (**IL-C_{16}**), [C_{12}Dabco]Br (**IL-C_{12}**), and N-butyl-4-aza-1-azaniabicyclo[2.2.2]octane bromide abbreviated [N-buDabco]Br (**IL-C_4**) (Scheme 1). The detailed synthesis conditions are shown in Table 1.

2. Experimental

2.1. Characterization

All the reagents were obtained from Merck or Aldrich and were used without further purifications. ^{1}H NMR spectra were recorded on either a Bruker DRX-250 (250 MHz) spectrometer in $CDCl_3$. Carbon nuclear magnetic resonance (^{13}C NMR) spectra were recorded on either a Bruker DRX-250 (62.9 MHz). The crystalline structures of the resultant samples were characterized by X-ray diffractometer (XRD, X'Pert Pro MPD, PANalytical) with Cu Kα radiation (40 kV and 40 mA). The FT-IR spectra were recorded using a Perkin-Elmer BX-II IR spectrometer. N_2 adsorption/desorption isotherms of samples were made at 77 K (BELSORP-mini II, MicrotracBEL, Corp.). The specific surface area and mesopore size distribution were determined by BET and BJH (Barrett–Joyner–Halenda) method, respectively [17].

2.2. Ionic liquid preparation

2.2.1. Hexadecyl-4-aza-1-azoniabicyclo[2.2.2]octane bromide (IL-C_{16})

To 17.8 mmol DABCO (98% Pure) in 50 mL AcOEt, 18.7 mmol 1-bromohexadecan was added, and the mixture was stirred at room temperature (r.t.) for 24 h. The product was filtered and then it was suspended into diethyl ether (30 cc) and stirred for one hour at r.t. The product was filtered and dried in vacuum to give the title compound (6.7 g, 90%).

^{1}H NMR ($CDCl_3$, 250 MHz,): δ = 0.80 (t, 3H, J = 6.75 Hz), 1.12–1.25 (m, 26H), 1.67–1.71 (m, 2H), 3.19 (t, 6H, J = 7.0 Hz), 3.36–3.42 (m, 2H), 3.60 (t, 6H, J = 7.5 Hz). ^{13}C NMR ($CDCl_3$, 62.9 MHz): δ = 13.99, 22.02, 22.52, 26.31, 29.09, 29.17, 29.31, 29.45, 31.74, 45.30, 52.37, 64.51.

2.2.2. Preparation of M-1

M-1 was synthesized utilizing CTAB and **IL-C_{16}** as dual template solution, and tetraethyl orthosilicate (TEOS) as a silica source. Ethylamine (EA) was used to regulate the pH of this solution. In a typical synthesis, Ethylamine was used to control the pH value of the aqueous solution, and CTAB and **IL-C_{16}** were used as a dual template. The needed quantity of TEOS was added drop-wise to the mixture. The mixed gel had the following molar constitutions: (SiO_2:CTAB:IL:EA:H_2O) = (1:0.2:0.2:0.6:100). After the TEOS was added, the solution was mixed-up firmly for two hours at r.t. The mixture was then moved into a stainless-steel autoclave and exposed to a high temperature at 373 K for 48 hours. The resultant product was washed with EtOH one time and then two times with deionized water. Then it was left to dry at a high heat of 373 K to get the product. The as-synthesized sample was then left in the air to get calcined for six hours at a temperature of 823 K and a heating rate **of 1 K** min^{-1}.

2.2.3. Preparation of K-1

K-1 was synthesized utilizing **IL-C_{16}** as template solution, and TEOS as a silica source. EA was used to regulate the pH of this solution. In a typical synthesis, Ethylamine was used to control the pH value of the aqueous solution. The needed quantity of TEOS was added drop-wise to the solution. The mixed gel had the following molar constitutions: (SiO_2:IL:EA:H_2O) = (1:0.4:0.6:100). After the TEOS was added, the solution was mixed-up firmly for two hours at room temperature. The mixture was then moved into a stainless-steel autoclave and exposed to a high temperature at 373 K for 48 hours. The resultant product was washed with EtOH a single time and then two times with deionized water. Then it was left to dry at a high heat of 373 K to get as-synthesized sample. The as-synthesized sample was then left in air to get calcined for six hours at a temperature of 823 K and a heating rate of 1 K min^{-1}.

2.2.4. Preparation of M-2 and K-2

M-2 and **K-2** were prepared based on our previous work [16].

3. Results And Discussion

Figure 1 illustrates the IR spectra of **K-1** and **M-1** materials. The bending modes of Si–O–Si bands are believed to cause the signals at 463–467 cm^{-1}. The symmetric/asymmetric stretching vibrations of Si-O-Si bonds are thought to lead to the bands at 799–804 cm^{-1} and 1064–1078 cm^{-1}, respectively. The asymmetric vibrations of (Si–OH) are presumably generating the signals at 953–965 cm^{-1}.The bending and stretching modes of adsorbed water molecules are believed to account for and contribute to the bands at 1640–1644 cm^{-1} and 3460–3465 cm^{-1}.

The small-angle XRD patterns of the products are shown in Fig. 2. **M-1** sample is related to the dual templates of CTAB and **IL-C_{16}**, and **M-2** sample is related to the only CTAB as template, **K-1** sample means only template **IL-C_{16}**, **K-2** sample used for the dual templates of CTAB and **IL-C_{12}**. XRD patterns of **M-1** indicated an intense sharp (100) peak, followed by minor (110) and (200) peaks, matching to a highly ordered hexagonal structure of MCM-41. XRD patterns confirm that by using dual templates, CTAB and IL, the crystallization of **M-1** increased in comparing with **M-2**. The (100) peak of **M-1** shift toward the slightly bigger angle, which shows the lattice space d_{100} of the pores ($d_{100} = \lambda/2\sin\theta$) became smaller. On the other hand, the low intensity and peak broadening detected in the XRD pattern of **K-1** and **K-2** indicate that these materials are not as well ordered as MCM- 41 and the structure array of their channels is disorder [18]. Two wide peaks which correspond to (100) and (200) diffraction in XRD pattern for **K-1** showed a more disordered structure than **K-2**. As the Fig. 2 showed, using the dual templates to produce **M-1** and **K-2** (Table 1, Entry 1 and 4) more ordered in comparing with one template (Table 1, Entry 2 and 3).

Nitrogen adsorption/desorption isotherms of samples show the typical type IV isotherm according to the IUPAC nomenclature for mesoporous structure (Fig. 3). The sharp inflection at $P/P_0 = 0.3–0.35$ in the isotherms of **M-1** sample indicates the narrow uniform mesoporous distribution. The existence of hysteresis loops in the **M-1** sample illustrates interaction network of porous structure which may be correlated to the existence of micropores, but **K-1** shows bigger hysteresis loop corresponds to the three-dimensional interconnection structure [19]. The sharp inflection p/p_0 in the isotherm **K-2** indicates the narrow uniform mesoporous distribution in comparing with **K-1** (Fig. SD. 3) [16].

Table 1 summarizes surface area and the pore volume of the characteristic MCM-41 and KIT-1 samples. The BET surface area of **M-1** is 1221 m^2/g, which is bigger than the value of 1028 m^2/g for **M-2** but BET surface area of **K-2** is 1012 m^2/g, which is bigger than about twice the value of 524 m^2/g for **K-1**. The specific surface area of the **K-2** (obtained by dual template) is upper 1000 $m^2\ g^{-1}$ and is also near to the ordered MCM-41.

The pore volume of **M-1** is 0.68 cm^3/g, which is smaller than the value of 1.03 cm^3/g for **M-2** and the pore volume of **K-1** is 0.55 cm^3/g, which is smaller than about half the value of 1.12 cm^3/g for **K-2**.

The pore size distribution of the mesopore and micropore of the products was obtained from desorption data using the BJH method (Fig. 4). **K-1** Sample shows non-uniform channels with 4–25 nm radiuses in

comparison to **M-1.** Fig. SD. 4 shows the TEM micrograph of **K-2** sample. It presents that the pore structure is the disorder network of short wormlike channel of mesoporous. These channels are connecting in a three dimensional with fairly uniform pore size [26]. Also the results confirm the ordered structure of **M-2** in comparing with the **M-1** and the **K-2** in comparing with the **K-1**. It seems using **IL-C_{16}** role is ordered micelles formation with CTAB. Only using **IL-C_{16}** with steric hindrance in cationic center lead to micelles formation that doesn't have good interaction with silicate polyanion in the polymerization process.

Wang et al. reported to investigation of 1-hexadecyl-3-methylimidazolium chloride (C_{16}mimCl) as template on synthesis of mesoporous silica in which the molar compositions of the mixed gel were: 1 TEOS: 0.543 C_{16}mimCl: 0.512 NaOH: 56 H_2O led to MCM-48 structure [20]. As we mentioned using only [C_{16}Dabco]Br without CTAB provide the disordered mesoporous system as KIT-1.

In continuing our previous researches, [6, 16] three cationic ILs based on DABCO with different chain length were applied as co-templates along with CTAB to produce micro-mesoporous silica materials. The using **IL-C_4** as co-template, showed good impact to prepare MCM-41 with higher interconnection network than using just CTAB [6]. The **IL-C_{12}** with the same molecular weight with CTAB in causes to form the KIT-1 micro-mesoporous system [16]. The **IL-C_{16}** with the similar to CTAB structure in the length of the alkyl side chain led to producing the micro-mesoporous MCM-41 with more order structure than comparison with only using CTAB (the present work). All of these synthesized mesoporous material has high surface area (Scheme 2).

4. Conclusion

In conclusion, using co-template in based on DABCO depend on length chain has different advantages like increasing interconnections, preparation with the disordered channel (KIT-1) and more ordered structure of mesoporous. Using only ILs led to KIT-1 with less order in comparing with the dual template. This work has completed the results of previous works about the effect of DABCO based ionic liquid in manufacture porous materials.

Declarations

Supplementary Data

Supplementary data associated with this article can be found, in the online supplementary content.

Author contributions

HS: Conceptualization; Methodology; Investigation; Writing. MS: Conceptualization; Visualization; Writing —review and editing and discussion. SP: Synthesis; Formal analysis.

Funding

The authors wish to thank the Ahvaz Branch, Islamic Azad University for providing the essential financial support.

Compliance with ethical standards

Conflict of interest The authors declare that they have no conflicts of interest.

Consent to participate Not applicable

Consent for publication Not applicable

References

[1] Machado SWM, Santana JC, Pedrosa AMG, Souza MJB, Coriolano ACF, Morais EKL (2018) Catalytic cracking of isopropylbenzene over hybrid HZSM-12/M41S (M41S = MCM-41 or MCM-48) micro-mesoporous materials, Pet. Sci. Technol., 36:923-929. doi: 10.1080/10916466.2018.1454950.

[2] Ryoo R, Kim JM, Ko CH, Shin CH (1996) Disordered molecular sieve with branched mesoporous channel network. J. Phys. Chem. 100:17718-17721 doi: 10.1021/jp9620835.

[3] Gholamzadeh P, Mohammadi Ziarani G, Badiei A (2017) Immobilization of lipases onto the SBA-15 mesoporous silica, Biocatal. Biotransfor. 35:131-150 doi: 10.1080/10242422.2017.1308495.

[4] Alothman ZAA (2012) review: fundamental aspects of silicate mesoporous materials. Materials. 5, 2874-2902 doi: 10.3390/ma5122874.

[5] Li Z, Zhang Y, Feng N (2019) Mesoporous silica nanoparticles: synthesis, classification, drug loading, pharmacokinetics, biocompatibility, and application in drug delivery, Expert Opin. Drug Deliv. 16:219-237 doi: 10.1080/17425247.2019.1575806.

[6] Sanaeishoar H, Sabbaghan M, Mohave F (2015) Synthesis and characterization of micro-mesoporous MCM-41 using various ionic liquids as co-templates. Micropor. Mesopor. Mat. 217:219-224 doi: 10.1016/j.micromeso.2015.06.027.

[7] Liu L, Xiong G, Wang X, Cheng X (2011) Synthesis of Nanosized AlKIT-1 Mesoporous Molecular Sieve and its Catalytic Performance for the Conversion of 1,2,4-Trimethylbenzene. Catal. Lett. 141:1136-1140 doi: 10.1007/s10562-011-0580-8.

[8] Roto R, Kartini I, Motuzas J, Triyana K, Siswanta D, Dwi Wahyuningsih T, Kusumaatmaja A (2019) Rapid Synthesis of MCM-41 from Rice Husk Using Ultrasonic Wave: Optimation of Sonication Time, Mater. Sci. Forum, *948*:198-205 doi: 10.4028/www.scientific.net/MSF.948.198.

[9] Coutino-Gonzalez E, Manriquez J, Robles I, Espejel-Ayala F (2018) Synthesis of MCM-41 material from acid mud generated in the aluminum extraction of kaolinite mineral. Enviro. Prog. Sustain.

Energy doi: 10.1002/ep.13069.

[10] Loganathan S, Kumar K, Ghoshal, AK (2019) Fabrication of Mesoporous Silica MCM-41 Via Sol-Gel and Hydrothermal Methods for Amine Grafting and CO_2 Capture Application, Urban Ecology, Water Quality and Climate Change, 38:341-349. doi: 10.1007/978-3-319-74494-0_26

[11] Azizi SN, Ghasemi S, Rangriz-Rostami O (2018) Synthesis of MCM-41 nanoparticles from stem of common reed ash silica and their application as substrate in electrooxidation of methanol Bull. Mater. Sci. 88:1-13 doi: 10.1007/s12034-018-1580-8

[12] Ryoo R, Kim JM, Shin CH, Lee JY (1997) Synthesis and hydrothermal stability of a disordered mesoporous molecular sieve. Stud. Surf. Sci. Catal. 105:45-52 doi: 10.1016/S0167-2991(97)80537-X

[13] Taubert A. (2016) Inorganic nanomaterials synthesis using ionic liquids, Encyclopedia of Inorganic and Bioinorganic Chemistry, 1-14 doi: 10.1002/9781119951438.eibc0355.pub2

[14] Li RX (2004) Green Solvents: Synthesis and Application of Ionic Liquids, Chemistry Technology Press, Beijing

[15] Isambert N, Duque MMS, Plaquevent JC, Genisson Y, Rodriguez J, Constantieux T (2011) Multicomponent reactions and ionic liquids: a perfect synergy for eco-compatible heterocyclic synthesis. Chem. Soc. Rev. 40:1347-1357 doi: 10.1039/C0CS00013B

[16] Sanaeishoar H, Sabbaghan M, Mohave F, Nazarpour R (2016) Disordered mesoporous KIT-1 synthesized by DABCO-based ionic liquid and its characterization. Micropor. Mesopor. Mat. 228:305-309 doi: 10.1016/j.micromeso.2016.04.003.

[17] Barrett EP, Joyne LG, Halenda PP (1951) The determination of pore volume and area distributions in porous substances. I. Computations from nitrogen isotherms. J. Am. Chem. Soc. 73:373-380 doi: 10.1021/ja01145a126.

[18] Yue Y, Sun Y, Gao Z (1997) Disordered mesoporous KIT-1 as a support for hydrodesulfurization catalysts. Catal. Lett. 47:167-171 doi: 10.1023/A:1019084400340.

[19] Gregg SJ, Sing KSW (11997) Adsorption, Surface Area and Porosity; Academic: London.

[20] Wang T, Kaper H, Antonietti M, Smarsly B (2007) Templating behavior of a long-chain ionic liquid in the hydrothermal synthesis of mesoporous silica. Langmuir, 23:1489-1495 doi: 10.1021/la062470y.

Tables

Table 1. The corresponding experimental conditions and textural properties of the samples.

Entry	Sample	IL	SiO_2:CTAB:IL	d_{100} (nm)	S_{BET} (m^2g^{-1})	V_{tot} (cm^3g^{-1})
1	**M-1**	C16[b]	1:0.2:0.2	3.74	1221	0.68
2	**M-2**[a]	-	1:0.4:0	3.83	1028	1.03
3	**K-1**	C16[b]	1:0:0.4	3.47	524	0.55
4	**K-2**[a]	C12[c]	1:0.2:0.2	4.01	1012	1.12

[a] Synthesis method and characterization of this sample were reported in Ref. 16.

[b] The same alkyl side chain length with CTAB

[c] The same molecular weight with CTAB

Figures

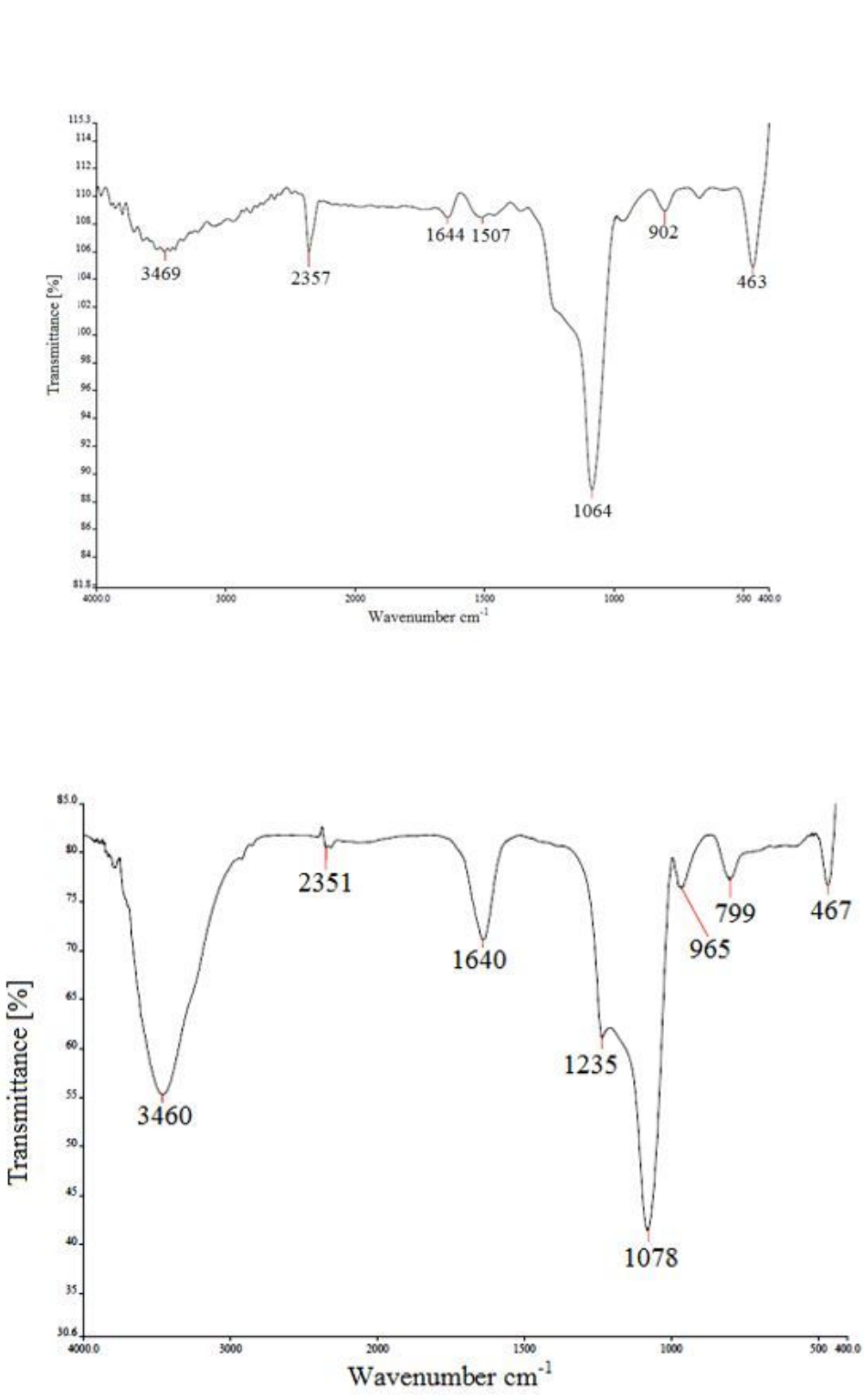

Figure 1

FT-IR spectra for a) M-1, b) K-1.

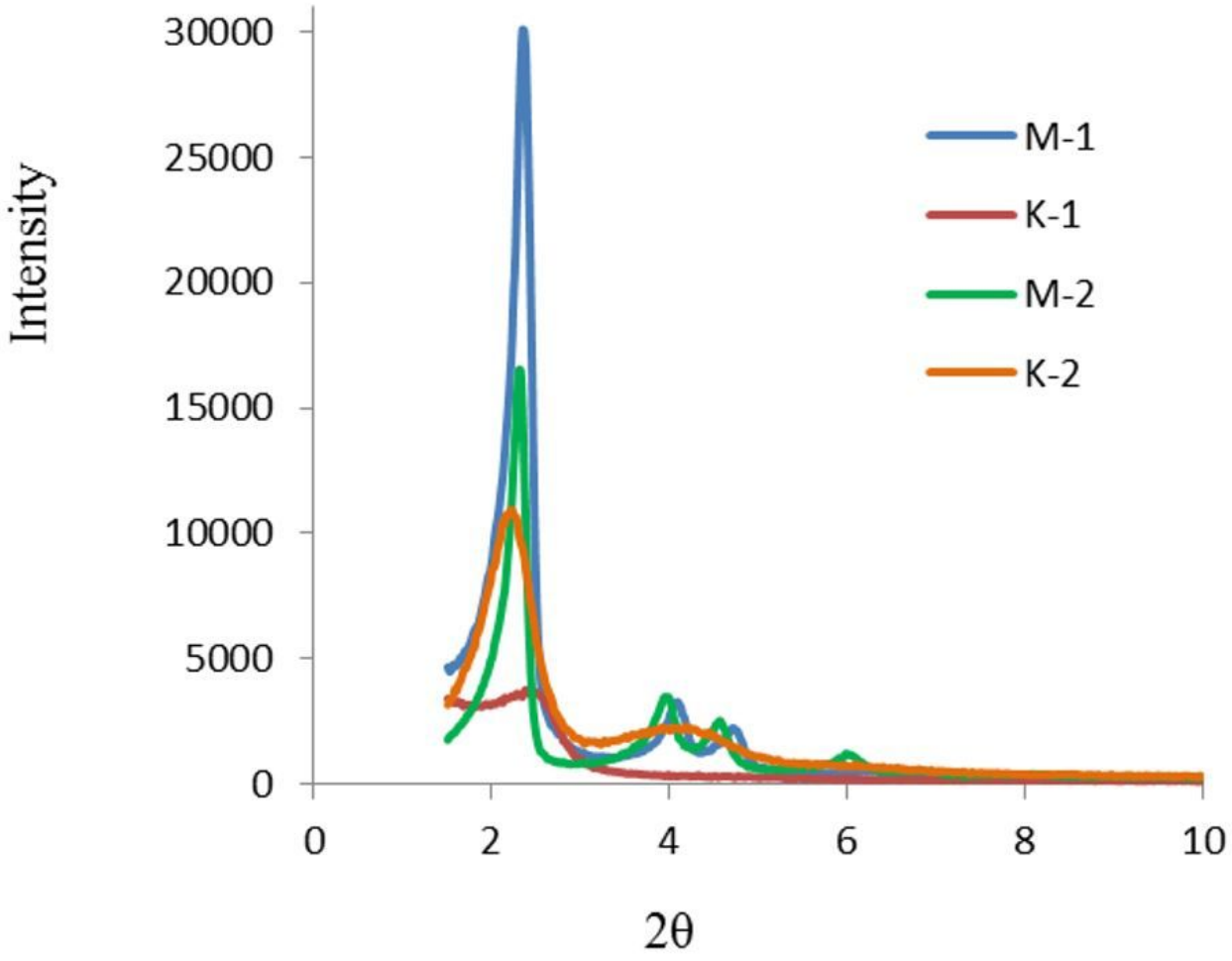

Figure 2

XRD for the M-1, M-2, K-1 and K-2.

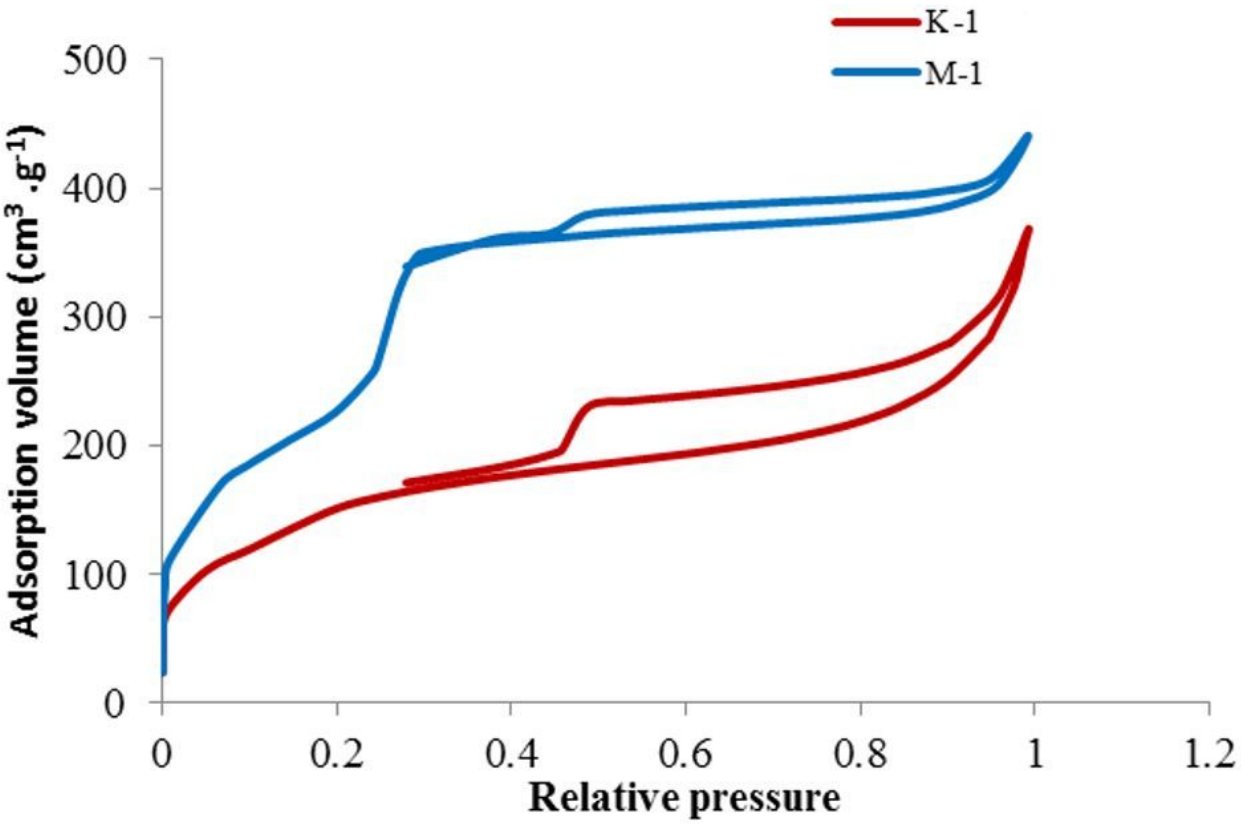

Figure 3

N2 adsorption-desorption isotherm curves of the synthesized solids.

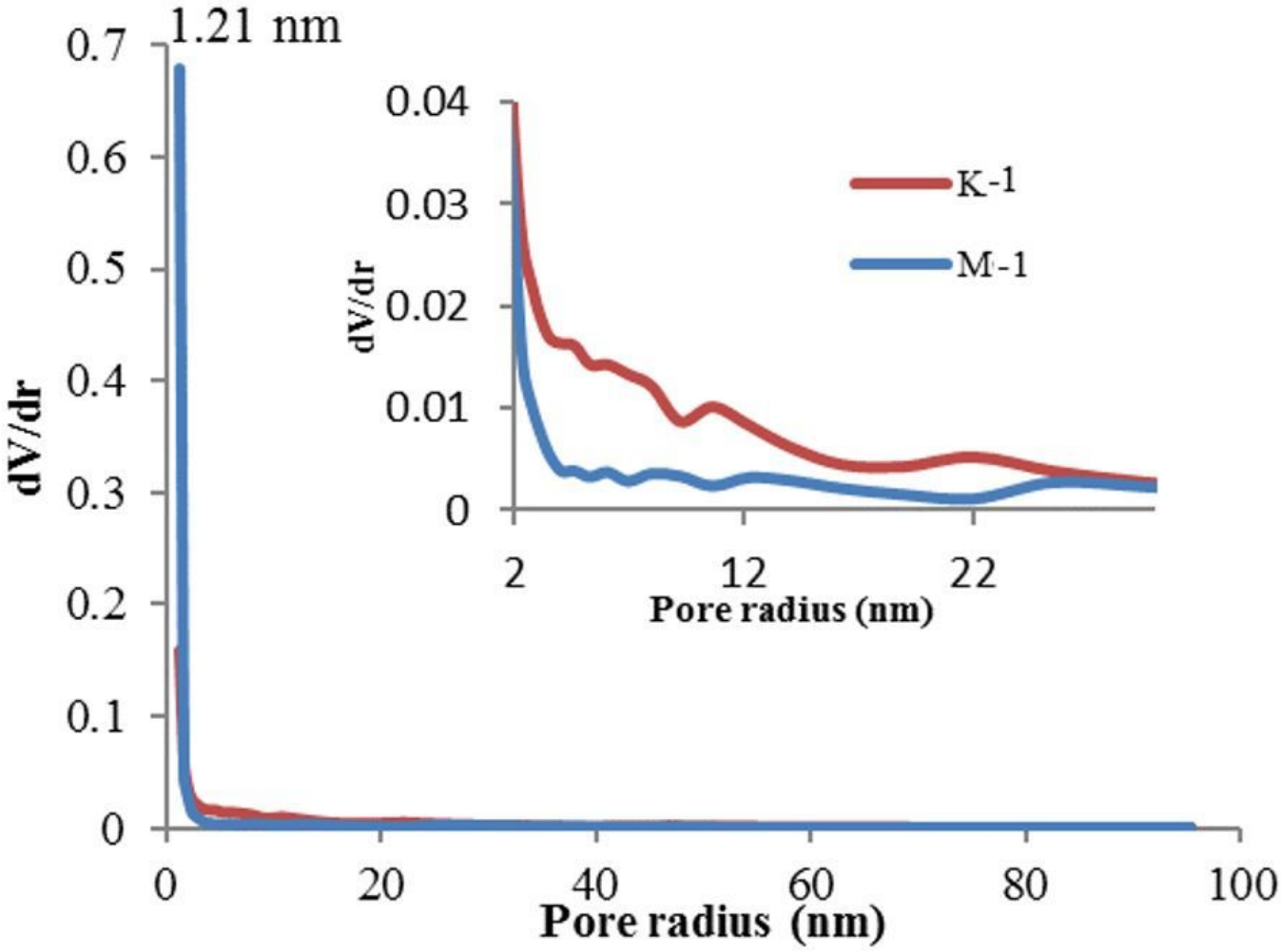

Figure 4

Pore size distribution (radius) for synthesized solids calculated by BJH method.

Supplementary Files

This is a list of supplementary files associated with this preprint. Click to download.

- scheme1.jpg
- scheme2.jpg
- GRAPHICALABSTRACT.docx
- supplementarydata.doc